

Supporting Information

Modular Off-Chip Emulsion Generator Enabled by a Revolving Needle

Yuxin Zhang¹, Qianbin Zhao², Dan Yuan², Hangrui Liu³, Guolin Yun², Hongda Lu², Ming Li⁴,
Jinhong Guo⁵, Weihua Li^{2*}, and Shi-Yang Tang^{1*}

¹*Department of Electronic, Electrical and Systems Engineering, University of Birmingham, Edgbaston, Birmingham, B15 2TT, UK.*

²*School of Mechanical, Materials, Mechatronic and Biomedical Engineering, University of Wollongong, Wollongong, NSW 2522, Australia*

³*ARC Centre of Excellence for Nanoscale BioPhotonics (CNBP), Department of Physics and Astronomy, Macquarie University, Sydney, NSW 2109, Australia*

⁴*School of Engineering, Macquarie University, Sydney, NSW 2122, Australia*

⁵*School of Information and Communication Engineering, University of Electronic Science and Technology of China, Chengdu, Sichuan Province 610051, China*

* Authors to whom correspondence should be addressed.

S.Tang@bham.ac.uk

weihuali@uow.edu.au

Table S1. Values of parameters used for numerical simulations.

Parameters	Value
<i>Viscosity of oil (η_{cp})</i>	30 mPa·s
<i>Density of oil (ρ_{cp})</i>	880 kg/m ³
<i>Viscosity of water (η_{dp})</i>	1 mPa·s
<i>Density of water ρ_{dp}</i>	1000 kg/m ³
<i>Interfacial tension (γ)</i>	8 mN/m (due to the presence of surfactant)
<i>Inner diameter of needle (D_{needle})</i>	60 μ m

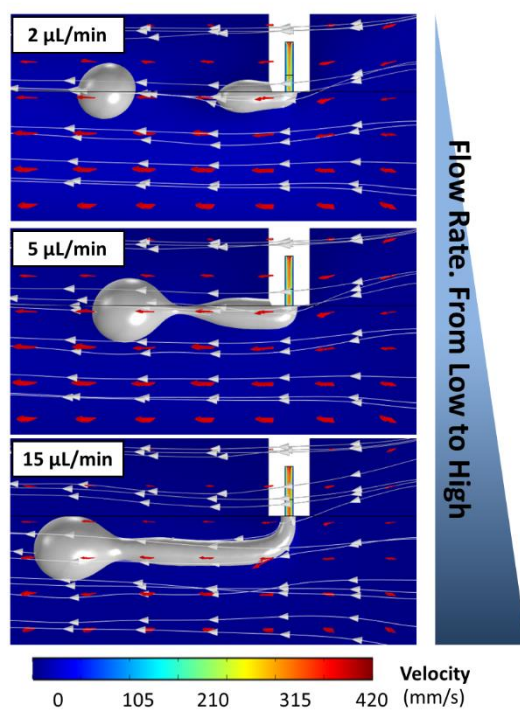


Figure S1. Simulation results for droplet size vs flow rate of the dispersed phase.

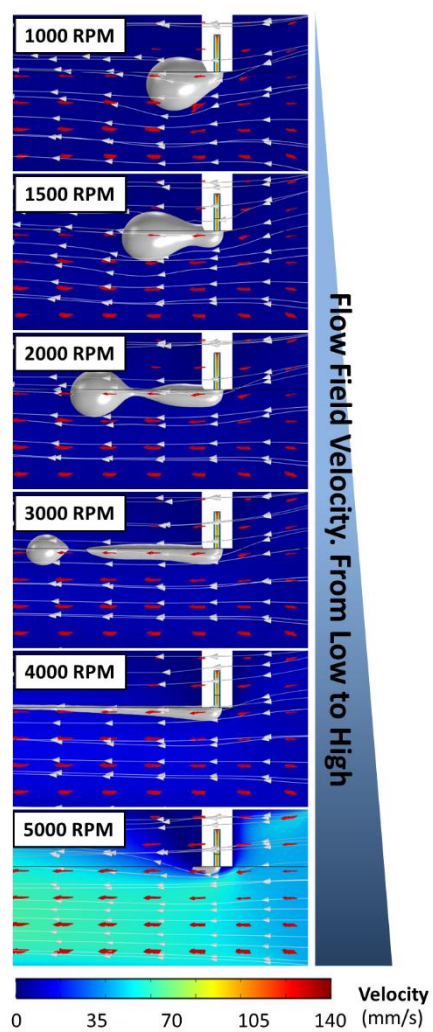


Figure S2. Simulation results for droplet size vs flow field velocity

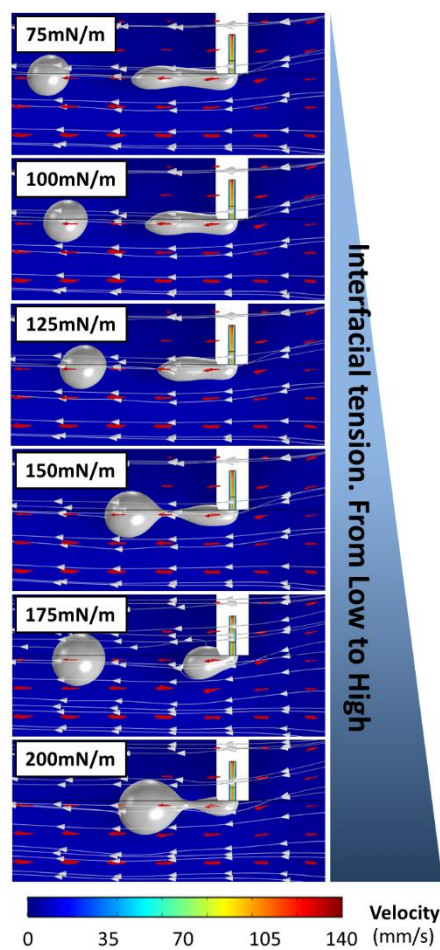


Figure S3. Simulation results for droplet size vs interfacial tension

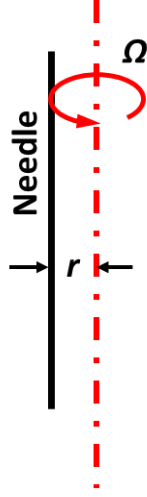


Figure S4. Schematic of the revolving needle.

The microdroplet production method used in our platform can be simplified to the case of droplet breakup in T-junction microfluidics channel. In this model, droplet breakup should occur when the drag force applied on the emerging droplet by the revolving needle overcomes the interfacial tension resisting deformation of the droplet¹. The dispersed phase inertia is negligible due to its relatively small Weber's number. The speed of the continuous phase flow v_{cp} induced by the revolving needle can be estimated as:

$$v_{cp} = \frac{2\pi r \Omega}{60} = \frac{\pi r \Omega}{30} \quad (\text{S1})$$

where Ω (RPM) is the revolving speed of the needle, and r is the distance from the needle tip to the axis of revolution (see Fig. S4). In the situation with low Reynolds number ($Re = \frac{\rho_{cp} v_{cp} D_{droplet}}{\eta_{cp}} \leq 1$), the drag force (F_{drag}) exerted on a spherical droplet is a modification of the Stokes formula and can be expressed as:

$$F_{drag} = 3\pi\eta_{cp}(v_{cp} - v_{droplet})D_{droplet} \quad (\text{S2})$$

where η_{cp} is the viscosity of the continuous phase liquid, $v_{droplet}$ is the droplet velocity, and $D_{droplet}$ is the droplet diameter. The capillary number Ca characterizing the relative importance of viscous

stresses and capillary pressure, and can be defined in terms of the continuous phase flow field that acts to deform the droplet:

$$Ca = \frac{\eta_{cp} v_{cp}}{\gamma} \quad (S3)$$

where γ is the interfacial tension. The interfacial tension would oppose the detachment of the droplet, and the interfacial tension force F_γ in our case can be calculated as:¹

$$F_\gamma = \pi \gamma \frac{D_{needle}^2}{D_{droplet}} \quad (S4)$$

where D_{needle} is the inner diameter of the needle used for the dispersed phase. Solving Equations S2-S4, we therefore can estimate of the droplet diameter $D_{droplet}$ as:

$$D_{droplet} = \sqrt{\frac{D_{needle}^2}{3Ca(1 - \beta)}} \quad (S5)$$

where β is the ratio between $v_{droplet}$ and v_{cp} (i.e. $\beta = v_{droplet}/v_{cp}$). Equation S5 indicates that the droplet diameter resulting from unconfined breakup is a function of the capillary number Ca , as well as the inner diameter of the needle.

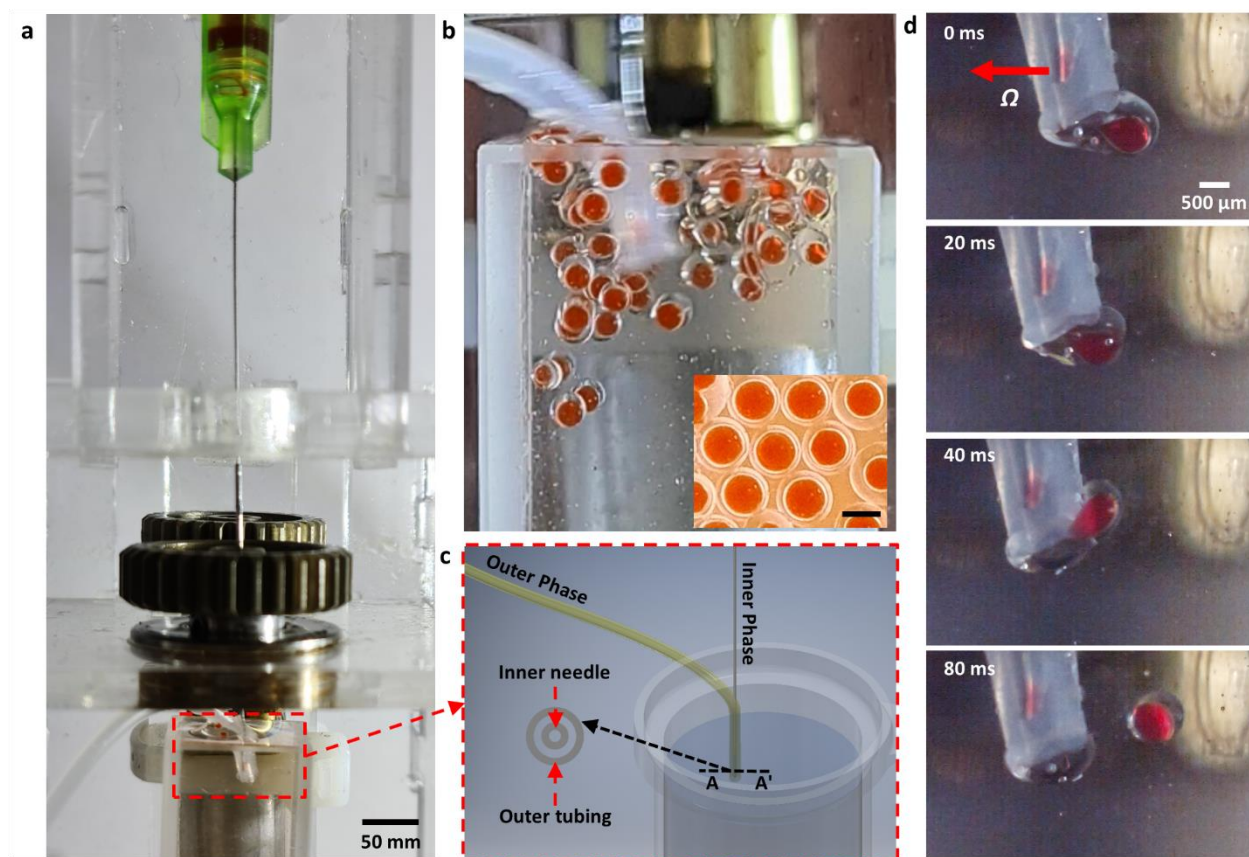


Figure S5. Illustration of the revolving needle emulsion generator (RNEG) for double emulsification. a) Actual image of the RNEG for double emulsification setup. b) Generation process for double emulsification in observing cuvette. The inset shows enlarged production of double emulsification. Scale bar is 500 μm . c) Zoomed-in schematic representation of the co-axis emulsification setup. d) Sequential snapshots showing the formation of w/o/w microdroplets using the RNEG (needle tip moves from right to left).

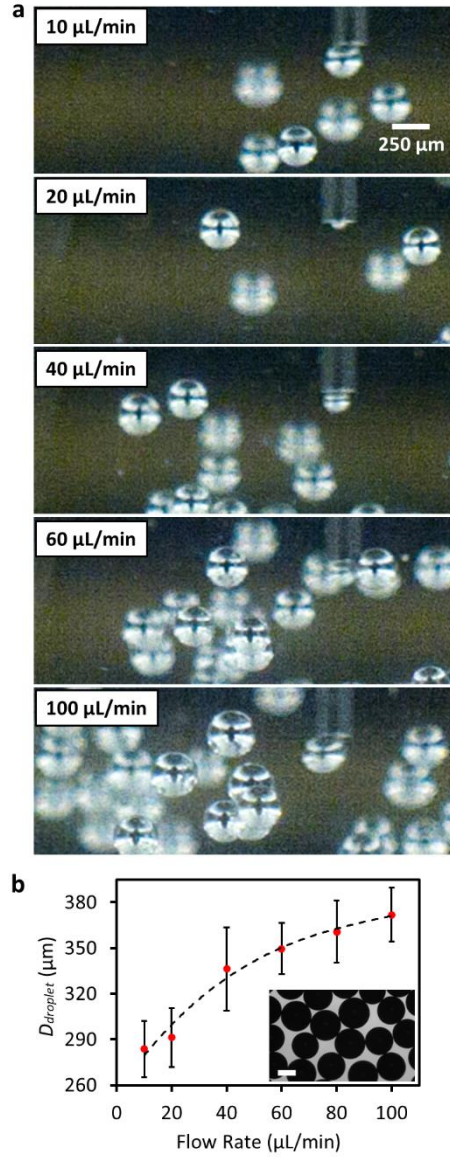


Figure S6. Production of EGaIn microdroplets using the RNEG. a) Images taken from a high-speed camera showing the production of liquid metal microdroplets at different flow rates. b) Plot of droplet diameter D_{droplet} vs Q . The inset image shows EGaIn droplet produced under the condition of at $\Omega = 3000$ RPM and $Q = 40 \mu\text{L}/\text{min}$.

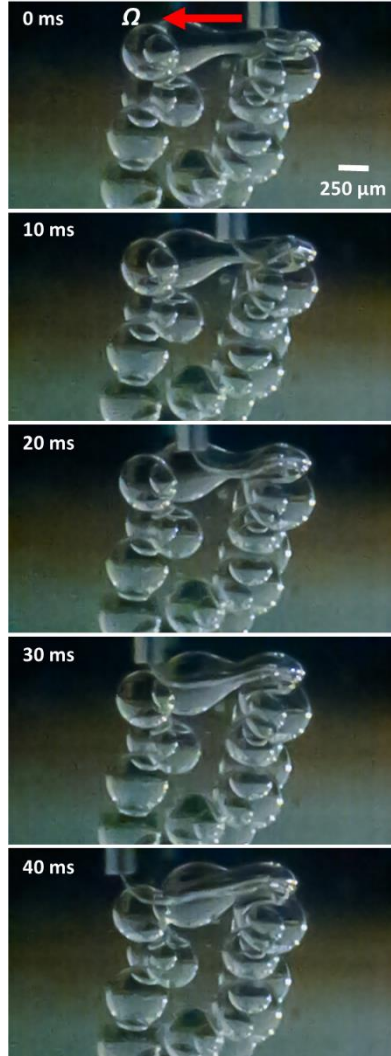


Figure S7. Sequential snapshots showing the jetting of PEGDA solution ($\Omega = 3000$ RPM and $Q = 200$ $\mu\text{L}/\text{min}$). Needle tip moves from right to left.

Table S2. Comparison of typical off-chip microdroplets generation techniques.

Technique	Throughput	Droplet diameter (μm)	Liquid	Ref (in main manuscript)
Centrifuges	Noncontinuous	~50~100	Aqueous droplets	6, 7
Capillary-based axisymmetric co-flowing device	0.1-2 $\mu\text{L}/\text{min}$	~30-230	Aqueous droplets	8
Spinning Conical Frustum	20-300 $\mu\text{L}/\text{min}$	~100-450	Aqueous droplets; EGaIn; Hydrogel particle	9
Off-the-shelf	20-200 $\mu\text{L}/\text{min}$	~170-400	PDMS droplets	10-12
Membrane-enabled	Noncontinuous	~25-200	Porous Silica Microparticles	13
Cross-interface	1-500nL/s	~30-80	Aqueous droplets	15
Yield-stress fluids enabled	50 $\mu\text{L}/\text{min}$	~250-1500	Aqueous droplets	19
Particle-templated	Noncontinuous	~40	Aqueous droplets	20
In-air ejection	Up to 2000 $\mu\text{L}/\text{min}$	~20-250	Hydrogel particle	21
This work	Up to 50 $\mu\text{L}/\text{min}$	~70-250	Aqueous droplets; EGaIn; Hydrogel particle	

Reference

1. J. Husny and J. J. Cooper-White, *Journal of Non-Newtonian Fluid Mechanics*, 2006, **137**, 121-136.